

# Studies on effects of pitting morphology in resistance spot welding of aluminium alloy

B. H. Chang<sup>\*1,2</sup>, D. Du<sup>1,2</sup>, Q. Chen<sup>1,2</sup> and Y. Zhou<sup>3</sup>

The effects of two types of electrode pitting morphologies, ring type and hole type, were investigated in resistance spot welding of aluminium alloy 5182 using both finite element analysis and physical modelling methods. Results showed that when using ring pitting electrode, the contact radius at faying surface is increased while the current distribution is not affected notably, and the nugget diameter is increased. When using hole pitting electrode, the contact radius at faying surface is increased further and the current density is decreased in the contact region. In addition, no current flows through the central part of faying surface under such conditions, consequently, central part does not melt and only donut shape nugget is formed. Hole type pitting poses more significant detrimental influence on joint quality than ring type pitting. These effects should be attributed to the distinct influences on contact status and therefore current distribution from electrodes of different pitting morphologies.

**Keywords:** Resistance spot welding, Pitting, Electrode degradation, Aluminium alloys, Finite element method

## Introduction

As a means to achieve vehicle emission and fuel economy objectives, reducing the weight of auto body has become a primary consideration in automotive industry. The aluminium alloys, with their low densities (one-third that of steel), high strength to mass ratio, resistance to corrosion and good recyclability, have been employed in manufacturing many new types of light-weight vehicles.<sup>1</sup> Resistance spot welding (RSW) is widely used in the production of aluminium body in white, and there are typically over 5000 spot welds in one auto body. However, the short electrode tip life has long been a major problem in resistance spot welding (RSW) of aluminium alloys. Electrode life is found to range from 400 to 900 welds in RSW of aluminium alloy 5182 with DC power supply, which is far below the electrode life when welding steels (over 2000 welds).<sup>2,3</sup> Frequent replacement or repairs are therefore necessary to guarantee the welding quality, which results in lower productivity in production line. Pitting at electrode tip surface has been considered as the main causes of electrode failure, because it will result in an increased contact area and hence a reduced current density at faying surfaces, which in turn lead to undersized nugget formation and hence a reduced joint strength.<sup>4</sup>

The pitting at electrode tip face could have different morphologies during service. Zhou *et al.*<sup>5</sup> have observed in their experiments that electrode pitting generally initiates at the edge regions of tip faces and, eventually, the pits grow and connect to each other forming roughly a ring pattern with a central contact area, as shown in Fig. 1a. This central contact area will continuously be pitted away during later welding and form a hole like pitting, as shown in Fig. 1b. Experiments have found that the central cavity is a much worse form of electrode pitting compared with a ring shaped pitting pattern, the authors' previous finite element analysis also has indicated that the diameter of the central cavity had significant effects on current distribution and hence nugget formation. All these results suggested that the tip face morphology can influence the weld quality. Nevertheless, it is so far not clarified that how the different electrode tip morphologies influence the welding process and in turn lead to different welding qualities.

In the present study, the two types of pitted electrodes shown in Fig. 1 are simulated by assuming premachined rings and holes. Finite element method is employed to study the effects of pitting morphologies on the mechanical contact condition, electric current distribution and nugget formation. The relationships among the mechanical, electrical and thermal factors are analysed comprehensively to reveal the fundamental causes for those effects. Experiments are also carried out to validate the computational results. This study is helpful in understanding the influence mechanism of electrode tip degradation on welding quality, establishing the electrode failure criterion, and furthermore can be beneficial in guiding the designing of electrode shape and materials to improve the electrode life.

<sup>1</sup>Department of Mechanical Engineering, Tsinghua University, Beijing, 100084, China

<sup>2</sup>Key Laboratory for Advanced Materials Processing Technology, Ministry of Education, China

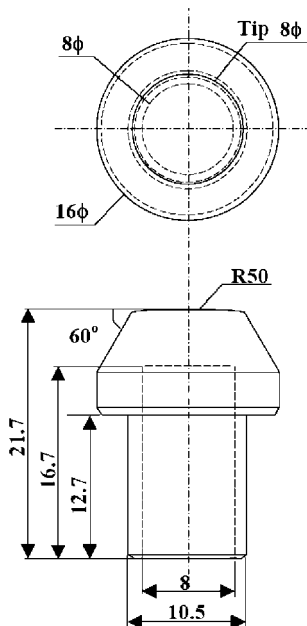
<sup>3</sup>Department of Mechanical Engineering, University of Waterloo, Waterloo, Ontario, N2L 3G1, Canada

\*Corresponding author, email bhchang@mail.tsinghua.edu.cn

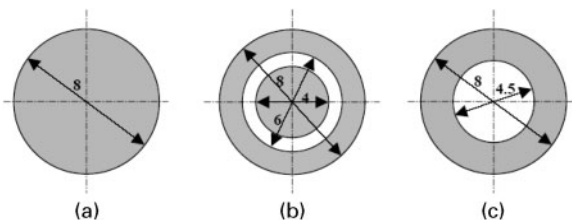


a ring type pitting; b hole type pitting

1 Two typical pitting morphologies



2 Configuration of original electrode (mm)



a new electrode; b ring type pitting; c hole type pitting

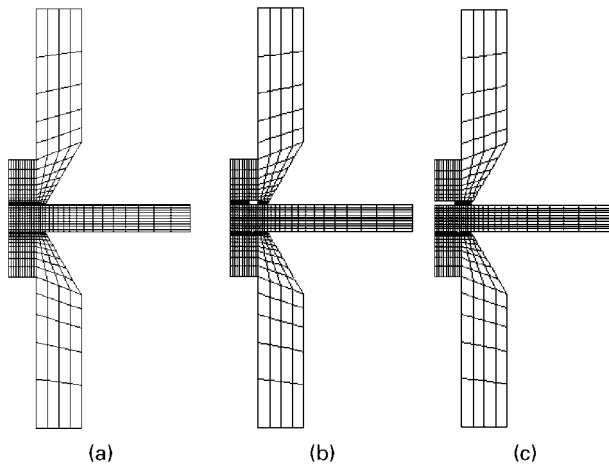
3 Three types of electrode tip face morphology

Materials and welding conditions

The aluminium alloy AA5182 sheet with a thickness of 1.5 mm, adopted widely in the fabrication of auto body, is used in the present study. The electrode is made of Cu-0.15%Zr alloy. The configuration of a new electrode without pitting is given in Fig. 2. To study the influences of electrode pitting morphology on welding quality, the two types of pitted electrodes shown in Fig. 1 are simulated by assuming premachined ring and hole at the electrode tip surface (see Fig. 3b and c) respectively.

Table 1 Welding conditions

Welding parameter	Value
Electrode force	5.3 kN
Welding current	34 kA (MFDC)
Welding time	5 cycles at 60 Hz
Holding time	12 cycles at 60 Hz
Base materials	AA5182
Electrode materials	Cu-0.15%Zr



a new electrode; b ring type pitting; c hole type pitting

4 Finite element meshes for three types of electrode tip face morphology

These two specially designed electrode tips can exclude the influence of pitting area by letting the ring and hole have the same area. The main attention can therefore be focused on the influence of different pitting morphologies in terms of shape and position (concentric hole and ring) in the present study. The welding conditions are the same for three electrodes as listed in Table 1.

Finite element analysis

Finite element analysis model

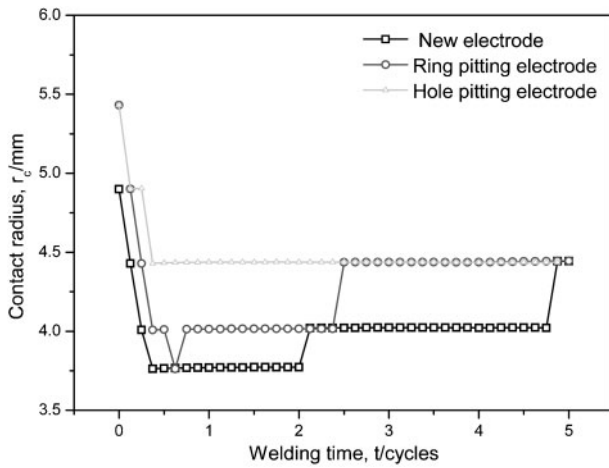
The Ansys/MP commercial finite element analysis code is employed in the present numerical analysis. Taking into account the axisymmetry created by the three types of electrodes in Fig. 3, resistance spot welding processes using three electrodes are simplified to axisymmetric problems. Figure 4 shows the axisymmetric finite element meshes used in the computations. Note in Fig. 4 that there is no pitting on bottom electrode for all three cases, because experimental researches from Peng et al.<sup>6</sup> shows that notable polarity effects exist when MFDC spot welder is employed, where the pitting is more significant on the top electrode (positive) than on the bottom electrode (negative).

The resistance spot welding is a complex process that involves strong coupling among multiple disciplines including electric, thermal, mechanical and even metallurgical phenomena. An incrementally coupled electrical-thermal-mechanical algorithm has been developed previously to incorporate all these coupling effects, in addition to the variation in current flow path caused by thermal expansion of workpieces.<sup>7</sup> Details of the algorithm and the contact resistance model based on the fundamental theory of electric contact used in finite element analysis are described in Ref. 7. All computations are performed on a Pentium IV personal computer. For each case, the computational time is ~ 2 h.

Finite element analysis results

Finite element analyses are performed with the model and welding conditions above mentioned. The computational results are presented below to demonstrate the influence of electrode pitting morphology on the mechanical, electrical and thermal behaviour during resistance spot welding.

Published by Maney Publishing (c) IOM Communications Ltd



**5 Variation of contact radii at workpiece/workpiece interfaces**

#### Variation of contact radius at faying surface

Figure 5 shows the variation of contact radius at faying surface (workpiece/workpiece interface) when three electrodes of different pitting morphologies are used. For the new electrode without pitting, the contact radius is  $\sim 4.89$  mm, greater than the nominal contact radius (electrode tip radius, 4.0 mm) at the beginning of welding process. For those two pitted electrodes, initial contact radii are both 5.43 mm, greater than that of new electrode. It is well known that the actual contact area at electrode/workpiece is basically not changed with electrode tip morphology under the same level of electrode force.<sup>4</sup> The pitted part cannot contact with workpiece, materials in a larger region will therefore come into contact, i.e. the nominal contact radius increases at electrode/workpiece interface. This in turn will lead to an increase in contact radius at faying surface.

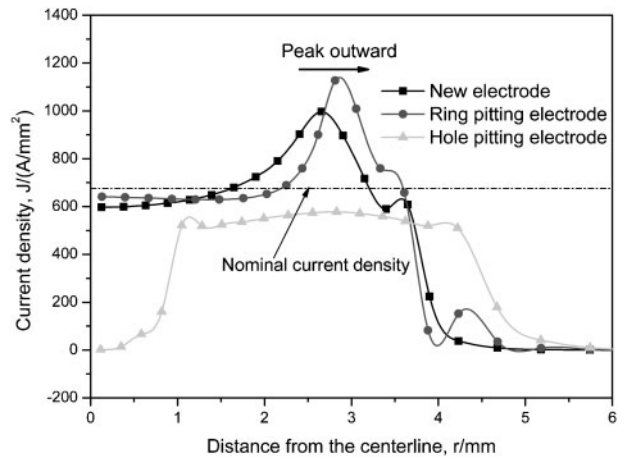
Within the first half cycle after welding process begins, contact radii for all three electrodes decrease immediately and reach minimum values respectively because of the thermal expansion of materials under heating at central part. The minimum contact radii are different for different electrodes. For the new electrode it is 3.75 mm, smaller than the other two cases. For the ring pitting electrode, although the minimum contact radius is the same as that for new electrode, it stays only within a very short period (0.25 cycle). Then it increases to a relatively stable value of  $\sim 4.0$  mm. For hole pitting electrode, the minimum contact radius is 4.44 mm. After the immediate decrease at the beginning, contact radii increase gradually during the following welding process for new and ring pitting electrodes, while for the hole pitting electrode, contact radius does not change any more.

In general, contact radius is the smallest for new electrode, the largest for hole pitting electrode, and in between for ring pitting electrode during the whole welding process.

#### Distribution of current density

Distribution of current density on the faying surface at the end of the second cycle is shown in Fig. 6 for three electrodes. The nominal current density, electric current divided by electrode tip area, is  $676.4 \text{ A mm}^{-2}$ , as a reference, it is also plotted in Fig. 6.

For the new electrode without pitting, current density distributes evenly at the centre of contact region. Peak



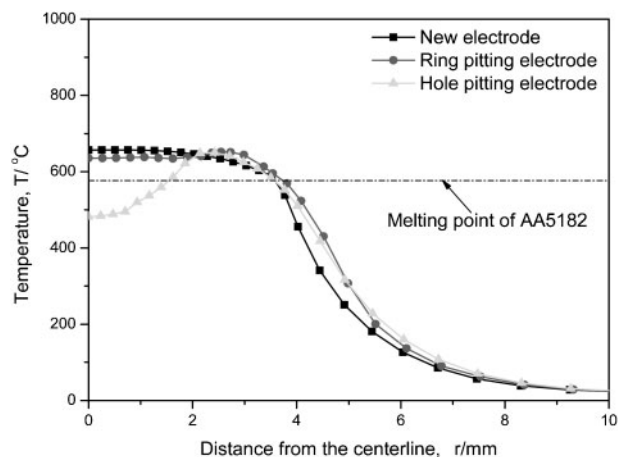
**6 Distribution of current density at workpiece/workpiece interface**

current density exists near the edge of contact region where the conduction area for electric current decreases and current lines tend to concentrate. Ring pitting does not notably affect the distribution pattern of current density, while it is worthy to note that the current density peak moves outward a little as a result of the slightly increased contact radius.

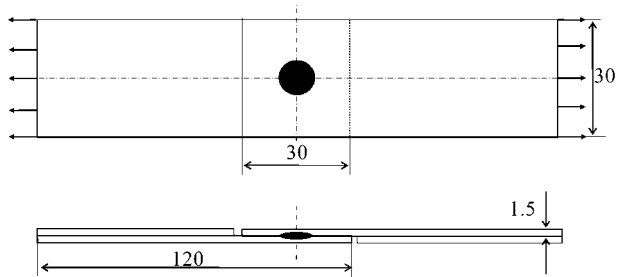
Current density distribution is significantly changed when the hole pitting electrode is used. Current distributes mainly within a ring ( $1.0 \text{ mm} \leq r \leq 4.25 \text{ mm}$ ). The current density is much lower in the central part with radius of 1.0 mm, and the current density is zero at the centre ( $r=0$ ), indicating there is no current flowing through. When the hole pitting is present, current will not flow through the pitted part any longer at the electrode/workpiece interface. Although the centre of faying surface is still in contact, and current can flow through at the beginning of welding ( $<1$  cycle), the current density at central part is smaller. The more significant thermal expansion of materials outside of the central region will push the central materials away from contact and hence cut off the electric current of that part during welding.

#### Distribution of temperature

Figure 7 presents the temperature distribution on the faying surface at the end of resistance spot welding for



**7 Distribution of temperature at workpiece/workpiece interface**



8 Shape and dimensions of overlapped spot welded joints (mm)

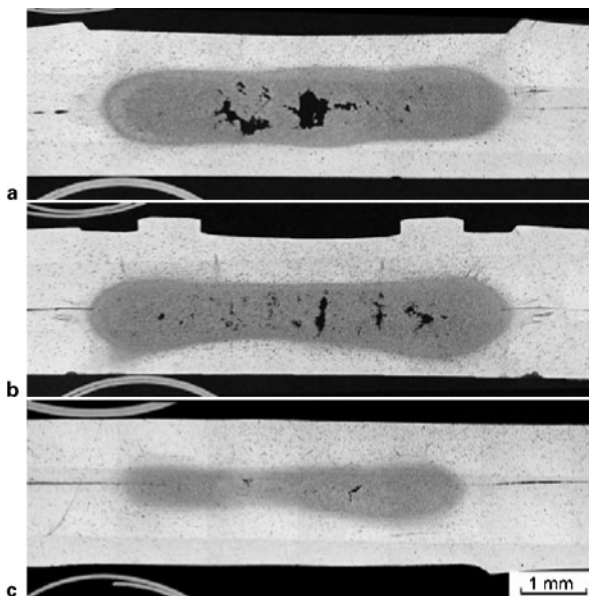
three electrodes. For the new electrode, temperatures are higher than the melting point of AA5182 (577°C) for the central region of  $r < 3.5$  mm, indicating the materials within this region is melted and a round nugget forms. When the ring pitting electrode is applied, melted region increases a little to  $r = 3.7$  mm, and temperature at centre decreases slightly, which indicating an increase in nugget diameter and thinning of nugget at centre. As shown before, comparing with the new electrode, the ring pitting will result in an increase in contact area at faying surface (~13.7%), which is not so significant as to bring notable influence on the distribution and magnitude of current density. Therefore, temperature at faying surface is not decreased notably while the region with temperature higher than melting point is increased as a result of the increased contact region, i.e. the nugget radius increases. When the hole pitting electrode is applied, temperatures at central part are lower than the melting point, and the melted materials are within the region of  $1.7 \text{ mm} < r < 3.5$  mm, indicating a ring shape nugget is formed. Referring to Figs. 5 and 6, it can be found that hole pitting will greatly increase the contact area (40.2%) and decrease current density at faying surface, which therefore lead to smaller melted region. Also, because the central part is separated and no electric current flow through, the temperature of that region is very low and materials are not melted. Only a ring shape thin nugget can formed under such conditions.

## Physical modelling

### Physical modelling procedures

Three types of electrodes, i.e. without pitting, with ring pitting and with hole pitting, are used to produce resistance spot welded joints of AA5182 under conditions listed in Table 1. The surface of the sheet material is covered with a light mineral oil. Because the sheet surface conditions are critical for welding quality in resistance spot welding of aluminium alloy, the surface is treated by applying alcohol and then acetone and then air dried before welding.

The shape and dimensions of the overlapped specimen produced are shown in Fig. 8. The samples are sectioned, polished and etched to observe the nugget shape under optical microscope. Tensile shear tests are carried out to obtain the joint strength. To avoid the bending of specimen during test caused by geometrical eccentricity, two aluminium plates with the same thickness of 1.5 mm are glued to the both ends of the specimen. After tensile shear tests, the diameters of the fractured nuggets are measured.



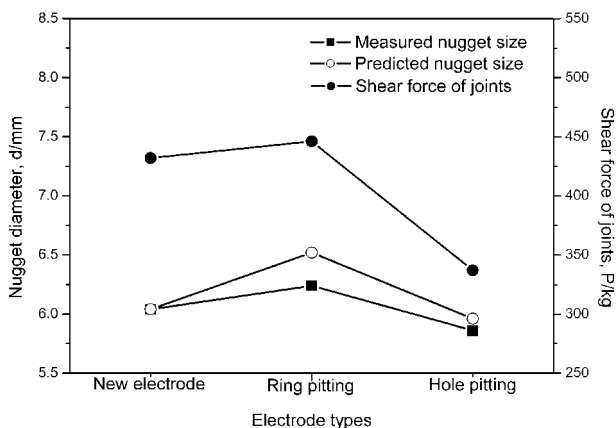
a new electrode; b ring type pitting; c hole type pitting  
9 Cross-sections of joints made with different electrodes

### Physical modelling results

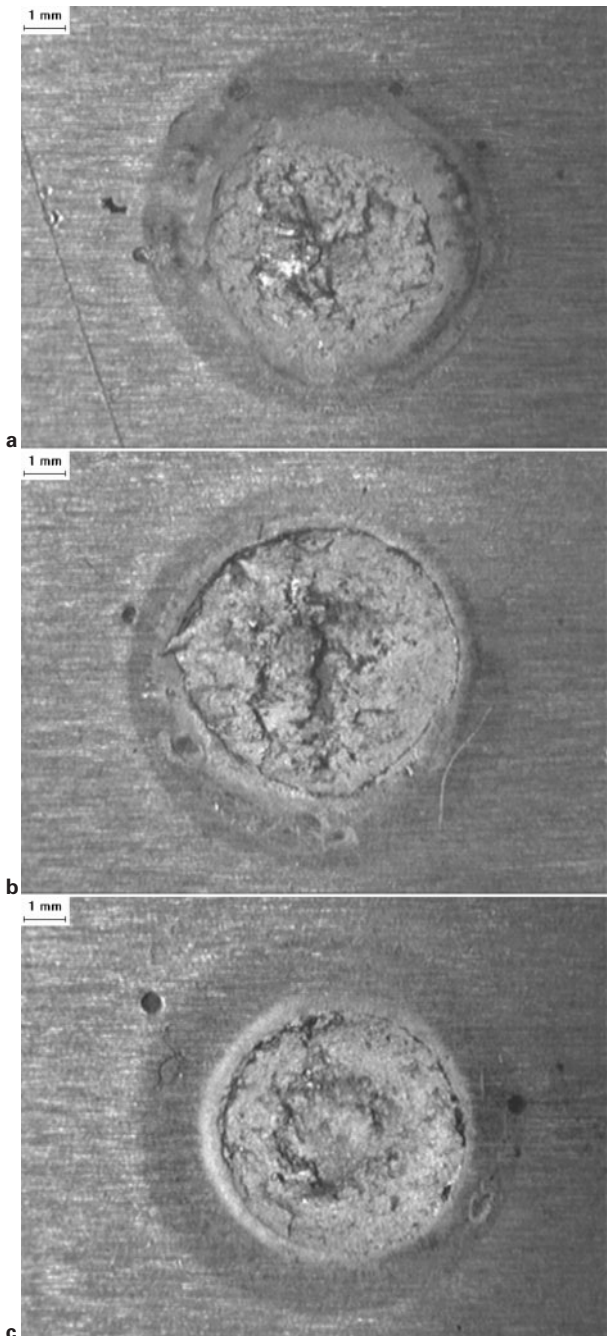
Figure 9 shows the cross-section of weld nuggets formed using three types of electrodes respectively. For new electrode without pitting, a complete nugget is obtained with basically same thickness at the middle part. A thinner nugget with a little larger diameter is formed for ring pitting electrode, and a much thinner ring shape nugget is formed for hole pitting electrode. Note the dark spots in all three weld nuggets, which are shrinkage porosities resulted from the solidification shrinkage of melted metals. The amount of shrinkage porosities should decrease with decreasing amount of melted metal. This explains why the shrinkage porosity amount decreases with the pitting corrosion, from ring to hole.

As the intrinsic discontinuities in aluminium alloy spot welds, the shrinkage porosities up to 40% of the weld diameter have no significant effect on joint strength.<sup>8</sup>

The nugget diameters are plotted in Fig. 10, which were measured from the fractured specimen (Fig. 11) after tensile shear tests. It should be pointed that in the shear tests, all specimens are interfacially fractured,



10 Shear strength and nugget diameter with different electrode morphologies



a new electrode; b Ring type pitting; c hole type pitting  
 11 Nuggets fractured by shear tests for three electrode morphologies

which is different from the fracture mode in cross-tension test, where the failure can change from interfacial (when the nugget is small) to pull-out. As shown in Fig. 10, the nugget diameter is a little (3.3%) larger when using ring pitting electrode, while it is a little (3.3%) smaller when using hole pitting electrode comparing with that of new electrode. Comparing the predicted (Fig. 7) with the measured nugget diameters given in Fig. 10, it can be seen that the actual nugget shape and dimensions agree well with numerical predictions. Minor overpredictions on the nugget diameters happen for the pitted electrodes, which could be the results of decreased precision in modelling the contact status at electrode/workpiece and workpiece/workpiece interfaces when pitting presents at electrode tip surface. Still, the

differences are within 4.5%, and numerical and experimental results are in pretty good agreement.

As far as the shear force of joint (Fig. 10) is concerned, it is increased by  $\sim 3.2\%$  owing to the small increase in nugget diameter when ring pitting forms at electrode tip. In contrast, the shear force of joint is decreased significantly by 22% when hole pitting electrode is used, although the nugget diameter changes very little. From finite element analysis results, it is found that although the hole pitting causes negligible influence on nugget diameter, the nugget is much thinner and also in ring shape, bonding strength is hence much lower than a complete nugget. Obviously, the shear force correlates very closely to the nugget shape and dimensions. The electrode life is generally defined as the weld number, and an electrode can produce before the joint strength is decreases to 80% of the initial strength of joints produced by a new electrode. According to this definition, the hole pitting electrode in the present study has already failed.

From the above analyses, it can be found that electrode pitting morphologies with the same area but different shapes and positions can have different effects on welding quality. When the pitting is in a ring shape, it brings little effects to welding quality. In contrast, when the pitting is in a hole shape, it brings notable detrimental effects to welding quality. Hence, when a hole type pitting occurs at electrode tip surface, it is necessary to take some measures to guarantee the joint strength, like replacement or repair of electrodes. This study presents a base to easily judge the electrode failure, and can be of significances in guiding the designing of electrode shape and materials to improve the electrode life.

## Conclusions

Using finite element analysis and physical modelling methods, the effects of electrode pitting morphology on welding quality in addition to the influencing mechanism are studied using specially designed electrode with machined ring shaped and hole shaped pitting, based on which the following conclusions can be drawn:

1. The contact radius is the smallest for new electrode, the largest for hole pitting electrode, and in between for ring pitting electrode during the whole resistance spot welding process.

2. Ring pitting does not notably affect the distribution pattern of current density, while the hole pitting makes the electric current distribute mainly within a ring and no longer flow through the central part.

3. When the ring pitting electrode is applied, nugget increases a little and the centre of nugget becomes thinner, when the hole pitting electrode is applied, materials of central part will not melt and only a ring shape nugget forms. Hole type pitting has a much greater detrimental influence on joint strength than ring type pitting.

4. Effects of electrode pitting morphology on welding quality should be attributed to the distinct influences on contact status and therefore current distribution from different types of electrodes.

## Acknowledgements

The financial support is gratefully acknowledged from the Scientific Foundation for Returned Overseas Chinese Scholars, Ministry of Education, China. The

authors would also like to acknowledge the funding and support from Auto21, one of the Networks of Centres of Excellence supported by the Canadian Government, the Ontario Research and Development Challenge Fund and Alcan Inc.

## References

1. H. J. Powell, A. Seeds, D. Boomer, D. Biggs, C. Rudd, G. Smith, K. Young and K. Lindsey: 'Foresight vehicle – advanced materials and structures thematic group (FASMAT): mission to the USA automotive industry', TWI Report no 12013/99, TWI, Cambridge, UK, 1999.
2. S. Fukumoto, I. Lum, E. Biro, D. R. Boomer and Y. Zhou: *Weld. J.*, 2003, **82**, (11), 307s–312s.
3. I. Lum, S. Fukumoto, E. Biro, D. R. Boomer and Y. Zhou: *Metall. Mater. Trans. A*, 2004, **35A**, (1), 217–226.
4. B. H. Chang, Y. Zhou, I. Lum and D. Du: *Sci. Technol. Weld. Join.*, 2005, **10**, (1), 61–66.
5. Y. Zhou, S. Fukumoto, J. Peng, C. T. Ji and L. Brown: *Mater. Sci. Technol.*, 2004, **20**, (10), 1226–1232.
6. J. Peng, S. Fukumoto, L. Brown and N. Zhou: *Sci. Technol. Weld. Join.*, 2004, **9**, (4), 331–336.
7. B. H. Chang, M. V. Li and Y. Zhou: *Sci. Technol. Weld. Join.*, 2001, **6**, (5), 273–280.
8. A. Gean, S. A. Westgate, J. C. Kucza and J. C. Ehrstrom: *Weld. J.*, 1999, **78**, (3), 80s–86s.